Journal of Alloys and Compounds 582 (2014) 6–11

Contents lists available at ScienceDirect

Journal of Alloys and Compounds

journal homepage: www.elsevier.com/locate/jalcom

NaAuS chicken-wire-like semiconductor: Electronic structure and optical properties

A.H. Reshak [a,b], Saleem Ayaz Khan [a,*], H. Kamarudin [b], Jiri Bila [c]

[a] Institute of Complex Systems, FFPW, CENAKVA, University of South Bohemia in CB, Nove Hrady 37333, Czech Republic
[b] Center of Excellence Geopolymer and Green Technology, School of Material Engineering, University Malaysia Perlis, 01007 Kangar, Perlis, Malaysia
[c] Department of Instrumentation and Control Engineering, Faculty of Mechanical Engineering, CTU in Prague, Technicka 4, 166 07 Prague 6, Czech Republic

ARTICLE INFO

Article history:
Received 18 May 2013
Received in revised form 30 July 2013
Accepted 31 July 2013
Available online 9 August 2013

Keywords:
Chicken-wire like
Electronic structure
Optical susceptibilities

ABSTRACT

The electronic structure, charge density and optical properties of NaAuS a chicken-wire-like semiconductor was calculated using full potential linear augmented plane wave based on density functional theory. The Ceperley-Alder local density approximation, Perdew Becke Ernzerhof Generalized gradient approximation and Engel Voskov Generalized Gradient Approximation were applied to solve the exchange correlation potential. The investigation of band structures and density of states elucidates that Engle Vasko Generalized Gradient Approximation shows close agreement to the experimental data. The calculated valence charge density shows pure ionic nature of Au–Au bond. It becomes partially covalent when Au is connected with two Na atoms. The linear optical susceptibilities of chicken-wire-like NaAuS semiconductor are calculated so as to obtain further insight into the electronic properties. The uniaxial anisotropy is −0.0005, indicating the strong anisotropy of the dielectric function in the NaAuS a chicken-wire-like semiconductor.

1. Introduction

The coinage metals contain d^{10} got significant interest due to its potential attractive d^{10}–d^{10} interactions which is still controversial and matter of a discussion marked [1].

The fascinating photochemical and photophysical properties of luminescent d^{10} compounds make them favorable for their possible applications in organic light emitting diode display technology [2]. Moreover there is electron deficiency in most of the hetero-atom-centered complexes and the gold–gold interactions give a substantial contribution to their stability [3]. Gold (Au) is notorious material in electronic packaging [4]. Cui et al. [5] extensively investigated the structural and mechanical stabilities of $AuAl_2$. Gold nanoclusters (AuNCs) also got considerable attention because of their good photostability, high fluorescence, excellent biocompatibility, non-toxicity, and solubility [6]. Recently incredible work have been done by Seryotkin et al. [7] by synthesizing gold–silver sulfoselenides from melts on heating stoichiometric mixtures of elementary substances in evacuated quartz ampoules which results a series of compounds i.e. $Ag_3AuSe_xS_{2-x}$ ($x = 0.25, 0.5, 0.75, 1, 1.5$).

In reaction with the molten polychalcogenide salt, gold losses its nobility and melts quickly at low temperature of 190 °C [8]. In early 1800 Bertholet [9] reported that gold dissolves in alkali metal poly sulfide melts but not in the molten sulfur. The chemical perspectives of ternary compounds AAuX (A = alkali metal; X = S, Se, Te) are very important because of many phases possibilities.

The strong affinity of gold for chalcogen atoms show the evidence in the reported ternary compounds $Cs_4Au_6S_5$ [10], $K_4Au_6S_5$ [11], contains long-chain polychalcogenides. Bakakin investigated the crystal structures of thirteen chalcogenides of Na, Au(I), and Ag(I) in the $Na_{2-x}(Au, Ag)_x(S, Se, Te)$ series, with $0 \leqslant x \leqslant 2$, from incorporated positions on the base of sphenoidal depiction. The joint dimensional effect and stoichiometric ratios of all components on the formation of filling rod positions was probed. New possibilities in crystal geometry and crystallochemical investigation of inorganic compounds whose structures are distinguished by a comparatively uniform distribution of atoms are proven as a prototype of chalcogenides [12].

Axtell et al. [13] synthesized LiAuS and NaAuS and discussed the structural and electronic properties including bond length and bond angles. They described that LiAuS and NaAuS, both of which feature infinite $(AuS)_n^{n-}$ chains in remarkable conformations and arrangements. The chains coil $(AuS)_n^{n-}$ in NaAuS become interlink and form layers like "chicken-wire" in an unusual fashion. This novel coiling mode allows Au–Au contacts to form, which help the structure to become stable.

To the best of our knowledge no comprehensive work neither experimental data on the optical properties or first principles calculations on the structural, electronic, and optical properties of chicken-wire-like NaAuS have appeared in the literatures.

* Corresponding author. Tel.: +420 777 083 956; fax: +420 386 361 219.
E-mail address: sayaz_usb@yahoo.com (S.A. Khan).

0925-8388/$ - see front matter © 2013 Published by Elsevier B.V.
http://dx.doi.org/10.1016/j.jallcom.2013.07.208

Therefore as a natural extension to previous experimental work of Axtell et al. [13] a detailed depiction of the structural, electronic, and optical properties of chicken-wire-like NaAuS using full potential method is timely and would bring us important insights in understanding the origin of the band structure and densities of states. Hence it is very important to use a full potential method. Present study is aimed towards such calculation using the full potential linear augmented plane wave (FP-LAPW) method which has proven to be one of the most accurate methods [14,15] for the computation of the electronic structure of solids within a framework density functional theory (DFT).

2. Crystal structure and method of calculation

The crystal structure of single molecule and crystal packing taken from relax geometry of present calculation are shown in Fig. 1a and b. As starting point of these calculations, the crystallographic data of chicken-wire-like NaAuS (space group Ccca, No. 68) semiconductor were taken from Axtell et al. [13] work. The crystal structure was optimized by minimization of the forces (1 mRy/au) acting on the atoms. The resulting relaxed geometry along with the experimental data is listed in Table 1. The electronic structure, electron space charge density, the chemical bonding and the optical properties were calculated at the relaxed geometry. The all electron full potential linear augmented plane wave (FPLAPW) method embodied in Wien2 K code [16] was used. The exchange correlation potential (XC) was treated by the local density approximation (LDA) Ceperley-Alder (CA) approach [17], Perdew Becke Ernzerhof Generalized Gradient Approximation (GGA-PBE) [18] and Engel Voskov Generalized Gradient Approximation (EVGGA) [19]. In order to converge the energy eigen values the wave function in the interstitial regions were expended in plane waves with cutoff $R_{MT}K_{max} = 7.0$. Where R_{MT} represent the muffin-tin (MT) sphere radius and K_{max} symbolize the magnitude of largest K vector in plane wave expansion. The muffin Tin (MT) sphere radii were selected to be 2.0 atomic units (a.u.) for Na, Au and S atom, respectively. For the structural optimization 35 k-points in the irreducible Brillouin zone were used. For the calculation of electronic properties 286 k-points were used. The self-consistent calculations are considered to be converged when the total energy of the system is stable within 10^{-5} Ry.

3. Result and discussion

3.1. Structural optimization

In order to investigate the ground state properties the total energy is calculated using GGA-PBE scheme. Fig. 2 shows the calculated total energies versus reduced volume for this compound. The calculated total energies are fitted to the Murnaghan's equation of state [20]:

$$E(tot) = \frac{B_0 V}{B_0'}\left[\frac{(V_0/V)^{B_0'}}{B_0' - 1} + 1\right] + E_0$$

to determine the ground state properties, where E_0, B_0 and B_0' symbolize ground state energy, volume, bulk modulus and pressure derivative of bulk modulus, respectively. The comparison of calculated optimize values of lattice parameters, atomic positions and E_0 with experimental data are shown in Table 1.

3.2. Band structure and density of state

The electronic band structure and the density of states were calculated using three kinds of XC shown in Figs. 3 and 4a. The calculated band structure shows that the conduction band minimum (CBM) is located at Γ centre of BZ, whereas the valence band maximum (VBM) is situated at T point of BZ, resulting in indirect band gap (T → Γ). The calculated energy gap is 1.97 eV (2.01 eV) using LDA (GGA-PBE) in comparison to the experimental ones (2.7 eV) [13]. It is well known that both of LDA and GGA-PBE usually underestimate the energy band gap. This is mainly due to the fact that they have simple forms that are not sufficiently flexible to accurately reproduce both the exchange–correlation energy and its charge derivative. Engel Voskov considered this shortcoming and

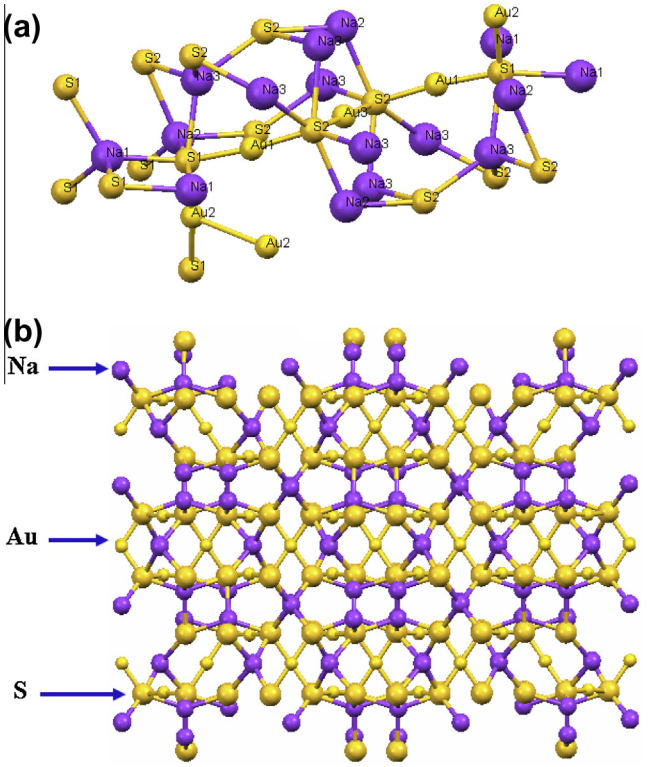

Fig. 1. (a) Molecular structure of NaAuS. (b) Packing of NaAuS chicken-wire-like semiconductor.

constructed a new functional form of GGA that is able to better reproduce the exchange potential at the expense of less agreement in the exchange energy. This approach, called EV-GGA, yields better band splitting and some other properties that mainly depend on the accuracy of the exchange–correlation potential [21–23]. Using EVGGA we have obtained better value of the energy gap (2.7 eV) in close agreement to the experimental band gap (2.7 eV). Therefore EVGGA is selected for further explanation of partial density of states (PDOS), electronic charge density and optical properties of the chicken-wire-like NaAuS. The partial density of states (PDOS) as illustrated in Fig. 4b–d, show that the low lying bands around −12.0 eV are mainly formed by Au-d, S-s states with negligible contribution of Au-S/p states. At energy ranges from −5.8 to −4.2 eV the formation of bands occurs by contribution of Au-s/p/d, S-s/p states and Na-s state, with small admixture of Au-p and Na-s/p. From −4.2 to −1.0 eV the Au-d and S-p show dominancy while the contribution of Au-s/p and Na-s/p states are minor. The valance band is formed by combination of Au-s/p and S-p states. In the conduction band Au-s/d and S-p states are foremost whereas Au-p, Na-s/p and S-s states show negligible contribution. From 5.5 to 8.0 eV the bands results from the contribution of Au-s/p and Na-s states, the Na-s state shows dominancy in this range. The highest occupied bands are originated from combination of Au-s/p/d, S-s/p and Na-s/p states. The Au-d and S-p states play leading role in this region.

The effective mass of electron ($m_e^* = 0.013m_e$), heavy holes ($m_{hh}^* = 0.045m_e$) and light holes ($m_{lh}^* = 0.037m_e$) were calculated which shows that the mobility of the holes in the valance band is substantially less than the mobility of electron in the conduction band.

3.3. Electronic charge density

Electronic charge density plot is used for accurate description of bonding nature [24,25]. The charge density contour plot in (001)

Table 1
Present optimized and experimental crystallographic data of NaAuS chicken-wire-like semiconductor.

	Crystallographic data		Atomic coordinates						
	Opt.	Exp.	Atom	X(Opt.)[a]	(Exp.)	Y(Opt.)[a]	(Exp.)	Z(Opt.)[a]	(Exp.)
a(Å)	14.811	14.658	Au1	0.118	0.122	0.373	0.373	0.219	0.219
b(Å)	21.262	21.043	Au2	0.000	0.000	0.250	0.250	0.465	0.471
c(Å)	07.192	07.118	Au3	0.000	0.000	0.500	0.500	0.000	0.000
V(Å^3)	2264.6	2195.0	S1	0.128	0.130	0.313	0.312	0.491	0.491
			S2	0.129	0.129	0.440	0.438	−0.040	0.491
			Na1	0.249	0.248	0.250	0.250	0.750	0.959
			Na2	1.000	0.000	0.138	0.138	0.750	0.750
			Na3	0.691	0.688	0.066	0.066	0.092	0.087

[a] Present work with GGA-PBE, Exp. [13].

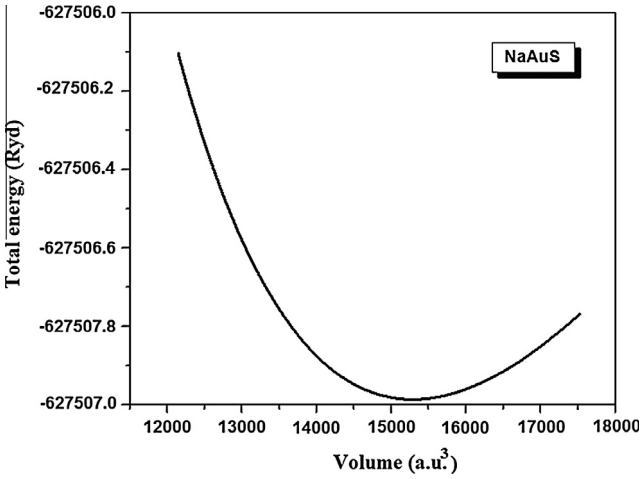

Fig. 2. Energy vs volume plot of NaAuS using GGA-PBE.

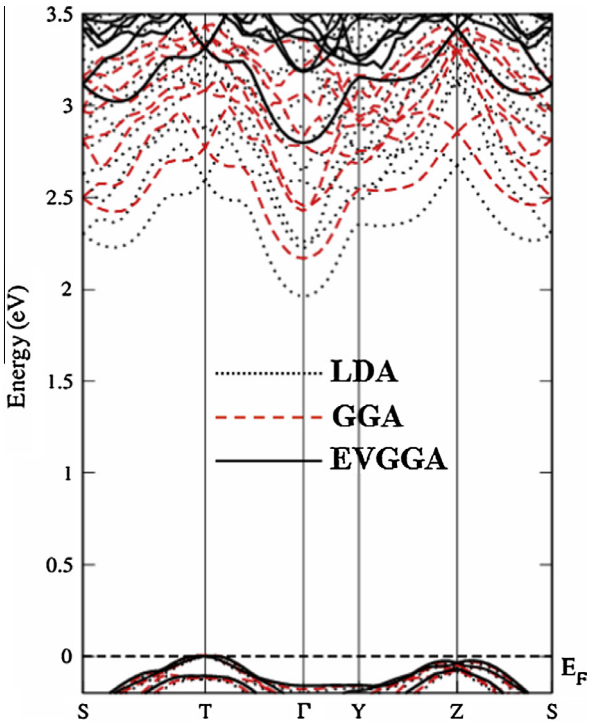

Fig. 3. Calculated band structure of NaAuS chicken-wire-like semiconductor.

crystallographic plane is shown in Fig. 5a. The electro-negativity difference of Au–S is very small (0.08) resulting in a strong non polar covalent bond. The Au atoms in (1 0 0) crystallographic plane (Fig. 5b) are independent from each other and exhibit a pure ionic nature as it is labeled by 1 and 2 in Fig. 5b. The Na–Au interactions maintain the weakly bonding characters. Following Fig. 5b, one can see that when two Na atoms form covalent bond with single Au atom, thus the Au share some charge with the nearest neighbor Au resulting in very weak covalent bond and strong ionic bond between Au–Au as it is labeled by 3 in Fig. 5b. The calculated bond lengths and angles of single molecule in Fig. 1a agrees well with experimental results of Axtell et al. [13] as shown in Tables 2 and 3.

3.4. Optical properties

Optical properties of the chicken-wire-like NaAuS semiconductor can be predicted from dispersion curves of dielectric function $\varepsilon(\omega)$. In this work the main aspect for calculating the optical properties is dispersion dielectric function. Energy eigenvalues and electron wave functions are needed for calculating of dispersion $\varepsilon(\omega)$. The energy eigen values and electron wave function are natural output from the calculation of the band structure. The crystal symmetry of the NaAuS structure allows three non-zero components of second order dielectric tensor along a, b and c crystallographic axis. The three principal complex tensor components for single crystals along $E\|x$, $E\|y$ and $E\|z$ are $\varepsilon^{xx}(\omega)$, $\varepsilon^{yy}(\omega)$ and $\varepsilon^{zz}(\omega)$. The three tensor components of the imaginary part of dielectric function are completely characterize the linear optical properties. These are calculated using the expression taken from Ref. [26]:

$$\varepsilon_2^{ij} = \frac{4\pi^2 e^2}{Vm^2\omega^2} \times \sum_{nn'\sigma} \langle kn\sigma|p_i|kn'\sigma\rangle\langle kn'\sigma|p_j|kn\sigma\rangle \times f_{kn}(1 - f_{kn'})\delta(E_{kn'} - E_{kn} - \hbar\omega) \quad (1)$$

In this expression m and e symbolize mass and charge of electron and ω represents the electromagnetic radiation striking the crystal, V stand for volume of the unit cell, in bracket notation p represents the momentum operator, $|kn\sigma\rangle$ represent the crystal wave function with crystal momentum k and σ spin which correspond to the eigenvalue E_{kn}. The Fermi distribution function is correspond to f_{kn} which makes sure the counting of transition from occupied to unoccupied states. The term $\delta(E_{kn'} - E_{kn} - \hbar\omega)$ shows the condition for conservation of total energy. The electron–phonon interaction play important role in calculated optical functions defining the broadening [27] and the multi-photons excitations [28]. In the present case the phonons have negligible contribution to $\varepsilon_2(\omega)$ therefore we ignore the phonons contribution involved in the indirect inter-band transition and only consider direct band transition between occupied and unoccupied states. The peaks in the optical response are caused by the allowed electric-dipole transitions between the valence and conduction

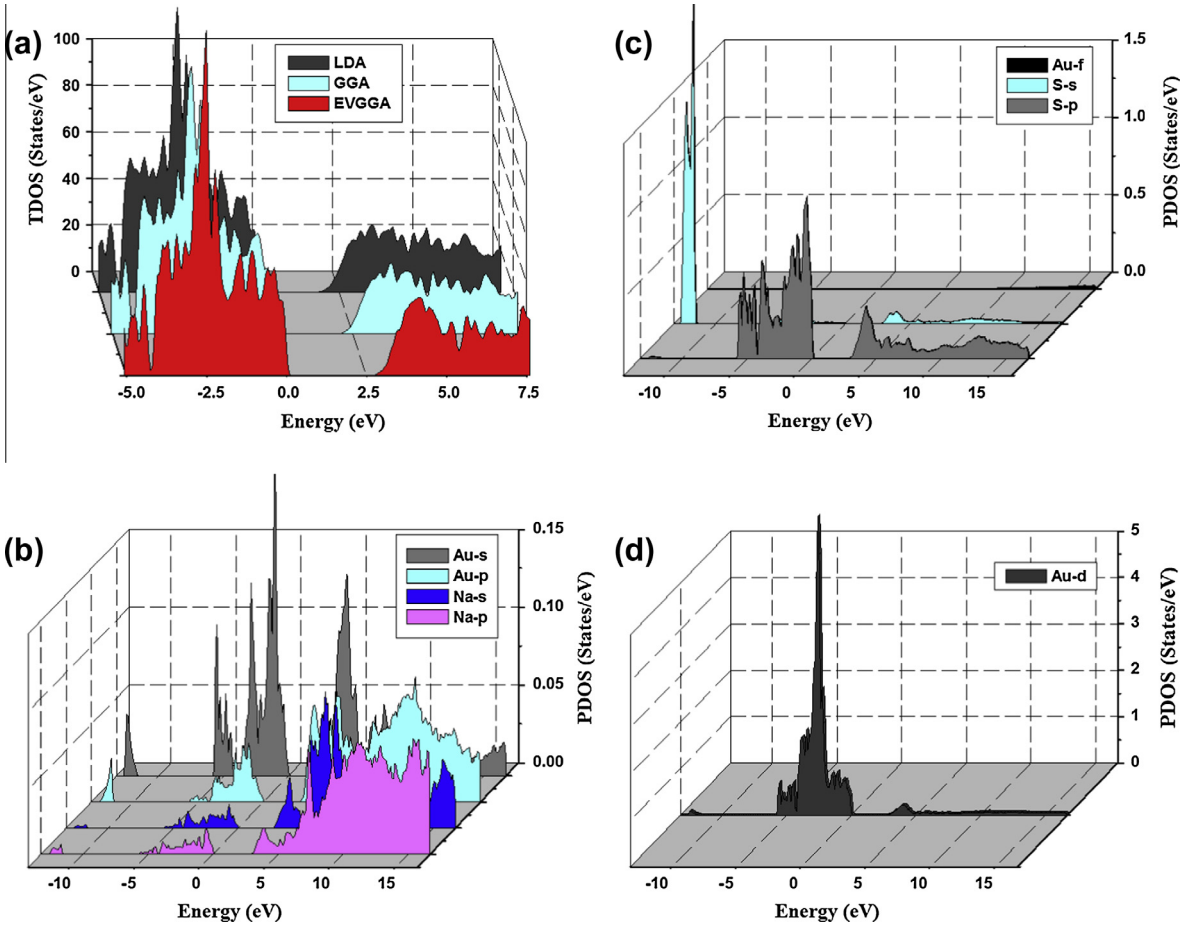

Fig. 4. Calculated total and partial densities of states (States/eV unit cell).

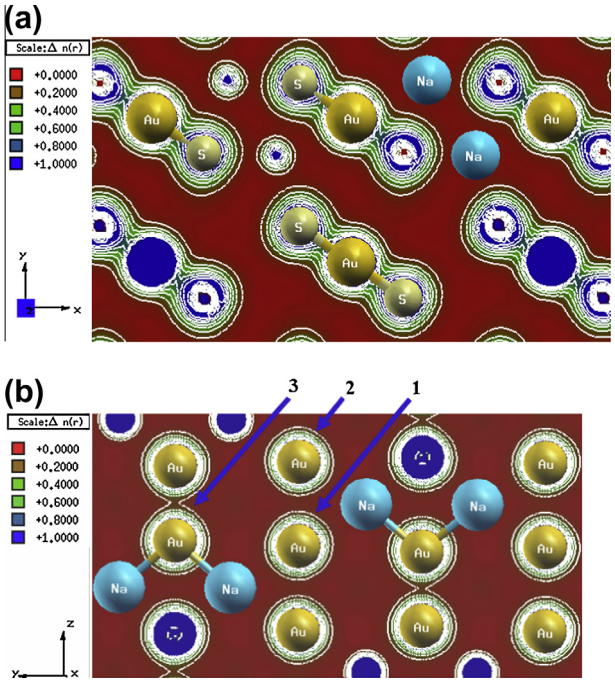

Fig. 5. Electronic charge density contour of NaAuS (a) in (001) plane and (b) in (100) plane.

Table 2
Calculated bond distances of NaAuS chicken-wire-like semiconductor.

Atom–atom	Present work[a] Distance (Å)	Exp. data Distance (Å)
Au2–Au2	3.14	3.06
Au1–S1	2.32	2.32
Au1–S2	2.31	2.32
Au2–S1	2.32	2.30
Au3–S2	2.31	2.31
Na1–S1	2.80	2.87
Na2–S1	2.85	2.82
Na2–S2	2.90	2.92
Na3–S1	2.80	2.81
Na3–S2	2.78	2.78

[a] Present work with GGA-PBE, Exp. Data [13].

Table 3
Calculated bond angles of NaAuS chicken-wire-like semiconductor.

Atom–atom–atom	Present work[a] Angle (°)	Exp. data Angle (°)
S1–Au1–S2	173.4	171.5
S1–Au2–S1	172.7	171.1
S2–Au3–S2	180	180
Au1–S1–Au2	102.6	101
Au1–S2–Au3	101.1	100
S1–Na1–S1	101.9	100
S1–Na2–S2	95.5	96.3
S2–Na2–S2	112.7	112
S1–Na3–S2	99.4	99

[a] gPresent work with GGA-PBE, Exp. Data [13].

bands. In order to identify these structures we need to look at the magnitude of the optical matrix elements. The observed structures would correspond to those transitions that have large optical matrix dipole transition elements.

The dispersion spectra of $\varepsilon_2(\omega)$ as illustrated in Fig. 6a, shows high transparency to electromagnetic (EM) waves up to 2.7 eV. Broadening is taken to be 0.1 eV which is typical of the experimental accuracy. The edge of optical absorption (fundamental absorption edge) for $\varepsilon_2^{xx}(\omega), \varepsilon_2^{yy}(\omega)$ and $\varepsilon_2^{zz}(\omega)$ are located at 2.7 eV. These edges of optical absorption give the threshold for direct optical transitions between the top of valence band and bottom of conduction band. The main structure of $\varepsilon_2^{xx}(\omega), \varepsilon_2^{yy}(\omega)$ and $\varepsilon_2^{zz}(\omega)$ which is situated between 4.0 till 7.0 eV, are corresponding to the transition from valence band maximum which is originated from Au-s/p and S-p states to the conduction band minimum that mainly formed by Au-s/d and S-p states. Fig. 6a, also reveals that there is isotropy among $\varepsilon_2^{xx}(\omega), \varepsilon_2^{yy}(\omega)$ and $\varepsilon_2^{zz}(\omega)$ in the spectrum range from 2.0 to 3.0 eV and from 10.3 till 13.6 eV. The main peaks of $\varepsilon_2^{xx}(\omega), \varepsilon_2^{yy}(\omega)$ and $\varepsilon_2^{zz}(\omega)$ are located at 5.1, 4.4 and 5.0 eV, respectively. In the energy range between 3.0 and 10.3 eV there exists a considerable anisotropy between the three polarizations.

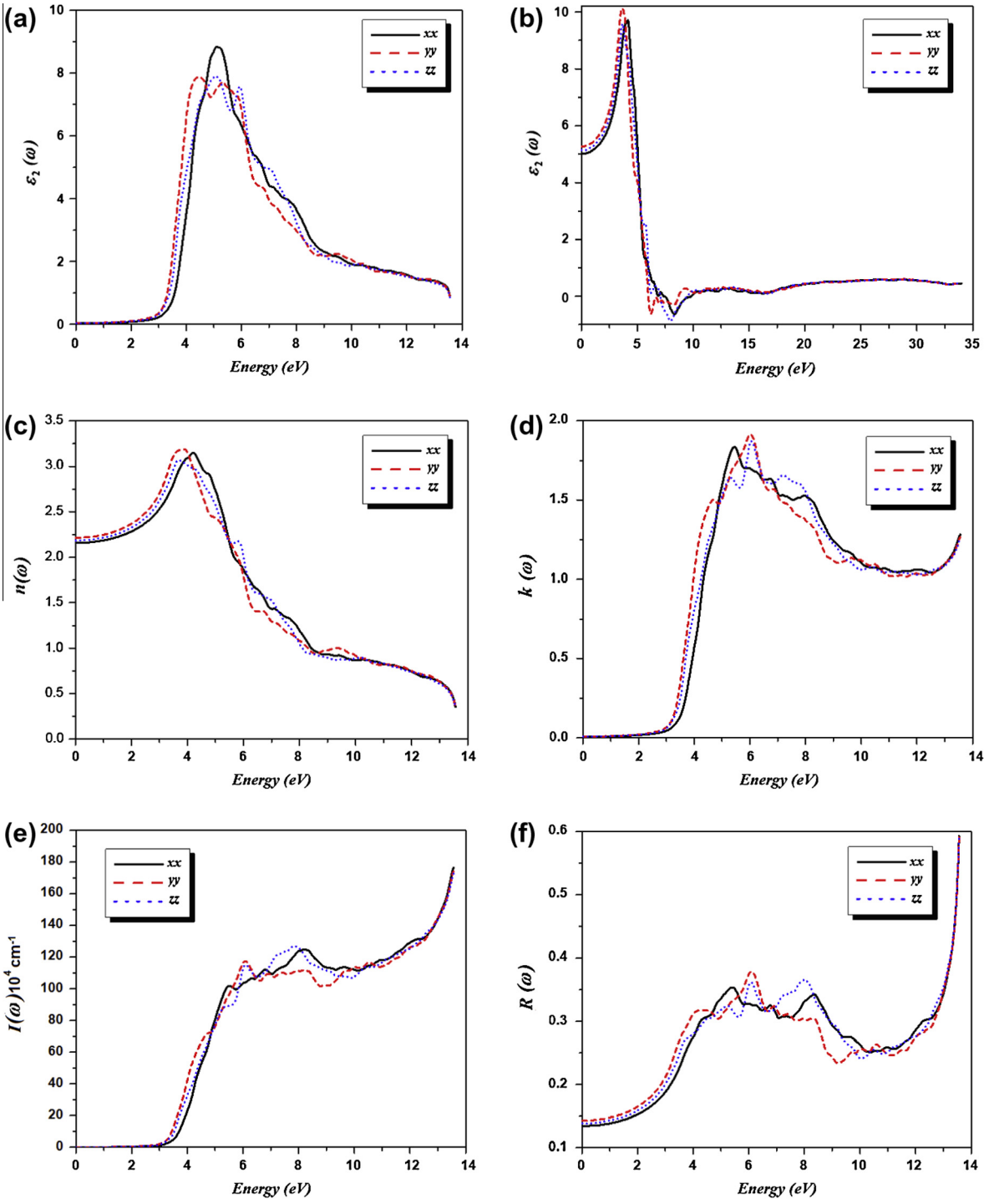

Fig. 6. (a) Calculated $\varepsilon_2^{xx}(\omega)$, $\varepsilon_2^{yy}(\omega)$ and $\varepsilon_2^{zz}(\omega)$. (b) Calculated $\varepsilon_1^{xx}(\omega)$, $\varepsilon_1^{yy}(\omega)$ and $\varepsilon_1^{zz}(\omega)$. (c) Calculated $n^{xx}(\omega)$, $n^{yy}(\omega)$ and $n^{zz}(\omega)$. (d) $k^{xx}(\omega)$, $k^{yy}(\omega)$ and $k^{zz}(\omega)$. ((e) Calculated $I^{xx}(\omega)$, $I^{yy}(\omega)$ and $I^{zz}(\omega)$. (f) Calculated $R^{xx}(\omega)$, $R^{yy}(\omega)$ and $R^{zz}(\omega)$. (g) Calculated $L^{xx}(\omega)$, $L^{yy}(\omega)$ and $L^{zz}(\omega)$.

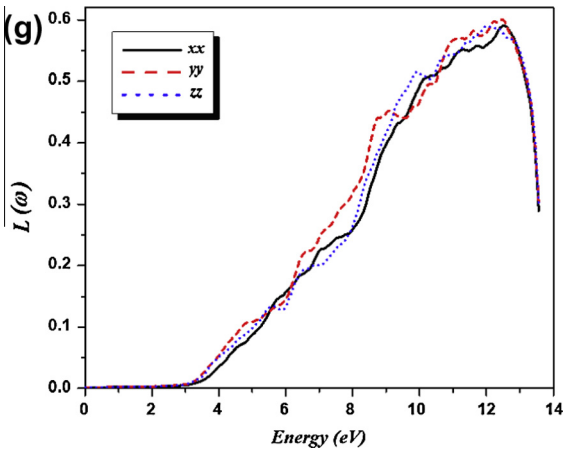

Fig. 6 (*continued*)

The real part of dispersion dielectric function can be calculated from imaginary part using Kramers–Kronig inversion [29]:

$$\varepsilon_1(\omega) = 1 + \frac{2}{\pi} P \int_0^{\infty} \frac{\omega' \varepsilon_2(\omega')}{\omega'^2 - \omega^2} d\omega' \qquad (2)$$

where P represents the principal value of integral. The calculated real part of dispersion dielectric function $\varepsilon_1(\omega)$ is shown in Fig. 6b. Again it show considerable anisotropy among $\varepsilon_1^{xx}(\omega)$,$\varepsilon_1^{yy}(\omega)$ and$\varepsilon_1^{zz}(\omega)$ except at 5.5 eV and the tail. The calculated optical dielectric constants at zero energy $\varepsilon_1^{xx}(0), \varepsilon_1^{yy}(0)$ and $\varepsilon_1^{zz}(0)$ are 4.65, 4.90 and 4.77 eV, respectively. The maximum peaks are located at 4.2 eV for $\varepsilon_1^{xx}(\omega)$ and 3.6 eV for $\varepsilon_1^{yy}(\omega)$and $\varepsilon_1^{zz}(\omega)$. The uniaxial anisotropy $\delta\varepsilon = [(\varepsilon_0^{II} - \varepsilon_0^{\perp})/\varepsilon_0^{tot}]$ is −0.0005, indicating the strong anisotropy [30] of the dielectric function in the NaAuS a chicken-wire-like semiconductor.

Using the calculated dispersion spectra of imaginary and real parts of dielectric function one can evaluate other optical properties such as refractive index $n(\omega)$, extension coefficient $k(\omega)$, absorption coefficient $I(\omega)$, reflectivity $R(\omega)$ and energy loss function $L(\omega)$. They are illustrated in Fig. 6c–g. The calculated non zero tensor components of static refractive index are 2.15, 2.21 and 2.18. Penn's model [31] elucidate that $\varepsilon_1(0)$ depends on band gap of the material and $\varepsilon_1(0)$ is directly related to the $n(0)$ by the relation $n(0) = \sqrt{\varepsilon_1(0)}$. Fig. 6f, shows the attenuation of EM waves in the material ranges from 2.7 to 13.5 eV. The maximum peaks of $k(\omega)$ along three polarization directions are located at 5.3, 6.0 and 6.1 eV. The absorption spectra of NaAuS show highest value at 13.5 eV correspond to the minimum value of $\varepsilon_1(\omega)$ shown in Fig. 6b. The three non zero components of $R(\omega)$ shows 13.1, 14.2 and 13.8 % reflection at 0.0 eV and reach to maximum value of 59 % at 13.5 eV. The $L(\omega)$ described the energy loss of fast electron traveling in the material. The sharp peaks produced in $L(\omega)$ around 12.5 eV are due to the plasma oscillation [32]. The above cases show considerable anisotropy among the three tensor components while for higher energy the three components show isotropic behavior.

4. Conclusions

A density functional theory (DFT) based on full potential linear augmented plane wave (FPLAPW) method was used for calculating the electronic structure, charge density and optical properties of the chicken-wire-like NaAuS semiconductor. The local density approximation (LDA) Ceperley-Alder (CA), Perdew Becke Ernzerhof Generalized Gradient Approximation (GGA-PBE) Engel Voskov Generalized Gradient Approximation (EVGGA) were applied to calculate the band structure, density of states and the optical properties. The investigation of the band structures and density of states confirm that EVGGA give energy gap value (2.7) close to the experimental one (2.7). The calculated valence charge density exhibits strong covalent bond between Au–S. There is pure ionic bond between Au–Au. When two Na atoms connected to Au, it become partially covalent and share some charge with neighboring Au. The calculated spectra of dielectric tensor components of imaginary part $\varepsilon_2(\omega)$, real part $\varepsilon_1(\omega)$, refractive index $n(\omega)$, extension coefficient $k(\omega)$, absorption coefficient $I(\omega)$, reflectivity $R(\omega)$ and energy loss function $L(\omega)$ belong to different polarization along $E\|xx$, $E\|yy$ and $E\|zz$ were discussed in detail. The calculated three non zero dispersion dielectric tensor components show considerable anisotropy among the three components.

Acknowledgements

This work was supported from the project CENAKVA (No. CZ.1.05/2.1.00/01.0024), the grant No. 134/2013/Z/104020 of the Grant Agency of the University of South Bohemia. School of Material Engineering, Malaysia University of Perlis, P.O Box 77, d/a Pejabat Pos Besar, 01007 Kangar, Perlis, Malaysia.

References

[1] P.K. Mehrotra, R. Hofmann, Inorg. Chem. 17 (1978) 2187–2189.
[2] Olga Crespo, M. Concepcion Gimeno, Antonio Laguna, Carmen Larraz, M. Dolores Villacampa, Chem. Eur. J. 13 (2007) 235–246.
[3] M. Concepción Gimeno, Antonio Laguna, Comments Inorg. Chem. 27 (2006) 127–143.
[4] Yee-wen Yen, Wei-kai Liou, Wan-ching Chen, Chao-wei Chiu, J. Alloys Comp. 574 (2013) 490–494.
[5] Shouxin Cui, Dong-Qing Wei, Qingming Zhang, Zizheng Gong, Hu Haiquan, J. Alloys Comp. 574 (2013) 486–489.
[6] Jing Lin, Zhijun Zhou, Zhiming Li, Chunlei Zhang, Xiansong Wang, Kan Wang, Guo Gao, Peng Huang, Daxiang Cui, Nanoscale Res. Lett. 8 (2013) 170.
[7] Yu.V. Seryotkin, G.A. Pal'yanova, N.E. Savva, Russ. Geol. Geophys. 54 (2013) 646–651.
[8] M.G. Kanatzidis, A.C. Sutorik, Prog. Inorg. Chem. 43 (1996) 151–265.
[9] C.L. Bertholet, Essai de Statique Chimique, 2nd Partie, Paris, 1803, pp. 437.
[10] P. Villars, K. Cenzual, J. Daams, R. Gladyshevskii, O. Shcherban, V. Dubenskyy, V. Kuprysyuk, O. Pavlyuk, I. Savysyuk, S. Stoyko, Landolt-Börnstein – Group III Condens. Matter 43A7 (2009) 701.
[11] P. Villars, K. Cenzual, J. Daams, R. Gladyshevskii, O. Shcherban, V. Dubenskyy, N. Melnichenko-Koblyuk, O. Pavlyuk, S. Stoiko, L. Sysa, Landolt-Börnstein – Group III Condens. Matter 43A3 (2006) 1.
[12] V.V. Bakakin, Crystallogr. Rep. 56 (6) (2011) 970–979.
[13] Enos Axtell III, Ju-Hsiou Liao, Mercouri G. Kanatzidis, Inorg. Chem. 37 (1998) 5583–5587.
[14] S. Gao, Comput. Phys. Commun. 153 (2003) 190–198.
[15] K. Schwarz, J. Solid State Chem. 176 (2003) 319–328.
[16] P. Blaha, K. Schwarz, G. Madsen, D. Kvasnicka, J. Luitz, WIEN2K, An Augmented plane Wave Plus Local Orbitals Program for Calculating Crystal properties, Vienna University of Technology, Austria), 2001, ISBN 3-9501031-1-2.
[17] D.M. Ceperley, B.I. Alder, Phys. Rev. Lett. 45 (1980) 566–569.
[18] J.P. Perdew, K. Burke, M. Ernzerhof, Phys. Rev. Lett. 77 (1996) 3865–3868.
[19] E. Engel, S.H. Voskov, Phys. Rev. B 47 (1993) 13164–13174.
[20] F.D. Murnaghan, Proc. Natl. Acad. Sci. USA 30 (1944) 244.
[21] A.H. Reshak, I.V. Kityk, R. Khenata, S. Auluck, J. Alloys Comp. 509 (2011) 6737–6750.
[22] A.H. Reshak, Dalibor Stys, S. Auluck, I.V. Kityk, Phys. Chem. Chem. Phys. 12 (2010) 2975–2980.
[23] A.H. Reshak, R. Khenata, I.V. Kityk, K.J. Plucinski, S. Auluck, J. Phys. Chem. B 113 (2009) 5803–5808.
[24] R. Hoffman, Rev. Mod. Phys. 60 (1988) 601–628.
[25] C.D. Gellatt, A.R. Willaims Jr., V.L. Moruzzi, Phys. Rev. B 27 (1983) 2005–2013.
[26] A. Delin, P. Ravindran, O. Eriksson, J.M. Wills, Int. J. Quantum Chem. 69 (1998) 349–358.
[27] M.I. Kolinko, I.V. Kityk, A.S. Krochuk, J. Phys. Chem. Solids 53 (1992) 1315–1320.
[28] K. Nouneh, I.V. Kityk, R. Viennois, S. Benet, S. Charar, S. Paschen, K. Ozga, Phy. Rev. B 73 (2006) 035329–035337.
[29] H. Tributsch, A. Naturforsch. 32A (1977) 972.
[30] A.H. Reshak, Xuean Chen, S. Auluck, I.V. Kityk, J. Chem. Phys. 129 (2008) 204111.
[31] D.R. Penn, Phys. Rev. B 128 (1962) 2093–2097.
[32] L. Marton, Rev. Mod. Phys. 28 (1956) 172–184.